Molecular Information of Charybdotoxin Blockade in the Large Conductance Calcium-activated Potassium Channel

Su Qiu,† Hong Yi,† Hui Liu, Zhijian Cao, Yingliang Wu,* and Wenxin Li*

State Key Laboratory of Virology, College of Life Sciences, Wuhan University, Wuhan, 430072, PR China

Received January 18, 2009

The scorpion toxin, charybdotoxin (ChTX), is the first identified peptide inhibitor for the large-conductance Ca^{2+} and voltage-dependent K^+ (BK) channel, and the chemical information of the interaction between ChTX and BK channel remains unclear today. Using combined computational methods, we obtained a ChTX-BK complex structure model, which correlated well with the mutagenesis data. In this complex, ChTX mainly used its β-sheet domains to associate the BK channel with a conserved pore-blocking Lys27. Another crucial Tyr36 residue of ChTX lied over the loop connecting selectivity filter and S6 helix of BK channel, forming a hydrogen bond with Gly291 of BK channel. Besides, the unique turret region of BK channel was found to be far away from bound ChTX, which could explain the fact that many BK channel blockers show less selectivity over Kv channels. Together, all these information is helpful to reveal the diverse interactions between scorpion toxins and potassium channels and can accelerate the molecular engineering of specific inhibitor design.

INTRODUCTION

Scorpion toxins constitute one of the largest potassium channel-modulator families.[1,2] These toxin peptides have been valuable molecular probes for studying the properties of K^+ channels, such as footprinting the pore structure topology, purifying specific channel proteins from native issues and elucidating their pharmacological characteristics.[3−5] Recently, our group utilized the computational and experimental methods to investigate the interactions between several scorpion toxins and potassium channels, and presented much helpful structural information on their interactions.[6−8] Scorpion toxin peptide BeKm-1 can specifically bind the hERG (human *ether-a-go-go*-related gene) potassium channel with an unusually long turret (S5 helix-pore helix linker). Structurally, the BeKm-1 mainly uses its helical region to associate the channel outer vestibule. The most critical Lys18 of BeKm-1 plugs its side chain into the channel selectivity filter. As for the hERG channel, four turrets form a "petunia" shape and keep far from bound BeKm-1 peptide.[6] Similar to the profile of hERG channel outer vestibule, the four turrets of Kv1.2 channel, with classical sequence length, are also in a decentralized state and far from bound peptide maurotoxin. This peptide mainly uses its β-sheet domains to associate the channel outer vestibule.[8] Recently, our studies also indicated that the turrets sometimes employed different conformational rearrangements when potassium channels were recognized by different scorpion toxins and their analogous peptides. From the interaction of designed ADWX-1 peptide with Kv1.1 and Kv1.3 channels, ADWX-1 peptide also mainly adopts its β-sheet domains as channel-interacting surface, and the four channel turrets are in the "half-open" state.[7,9] The turret in the A and C chains closely contact ADWX-1 peptide and strongly affect ADWX-1 selectivity between Kv1.1 and Kv1.3 channels, and the turrets in the B and D chains are far away from ADWX-1 and become less effect on the ADWX-1 selective binding. All above progresses of scorpion toxin-potassium channel interaction are accelerating to explore more structural information on scorpion toxin-potassium channel interactions.

Charybdotoxin (ChTX), a 37-residue peptide derived from the venom of the scorpion *Leiurus quinquestriatus hebraeus*,[10] is the first identified BK channel inhibitor.[11] Some mutant experiments have been used to map the function sites of ChTX for blocking BK channel.[11,12] However, the interaction details of functional residues between ChTX and BK channel remain unclear. With the help of ChTX as a molecular probe, we recently obtained the conformation switch information of channel turret when the large conductance Ca^{2+} and voltage-dependent potassium channel (BK channel) was coassembled with auxiliary β4 subunits or not.[13] When BK channel does not coassemble with β4 subunits, the four turrets keep decentralized state. After BK channel coassembles with β4 subunits, the four turrets keep "half-open" state and associate with four β4 subunits through electrostatic interactions. In company with previous work, we presented the detailed structure information on the ChTX-BK channel interaction in this work. The information is helpful to reveal the diverse interactions between scorpion toxins and potassium channels, based on which the molecular engineering of specific inhibitor design will be accelerated near the future.

MATERIALS AND METHODS

Atomic Coordinates and Protein−Protein Docking. The atomic coordinates of BK channel was obtained through segment-assembly homology modeling in our previous work.[6] The atomic coordinates of ChTX peptide (PDB code 2CRD) were downloaded from the Protein Data Bank.[14]

ZDOCK program, a fast Fourier transform (FFT)-based, initial-stage rigid-body molecular docking algorithm,[15] was

* To whom correspondence should be addressed. E-mail: ylwu@whu.edu.cn (Y.W.); liwxlab@whu.edu.cn (W.L.). Tel: ++86-(0)-27-68752831. Fax: ++86-(0)-27-68752146.

† These authors contributed equally to the work.

10.1021/ci900025n CCC: $40.75
Published on Web 06/05/2009

applied for predicting ChTX-BK channel interaction. All 12 ChTX conformations from NMR and the modeled BK channel structure were used to improve the rigid docking performance. For each group of docking results, clustering analysis and screening with the application of experimental information[11,12] were utilized for selecting possible hits. To identify appropriate candidate complexes for further MD simulations, a 500 steps energy minimization using SANDER module in the AMBER 8 suit of programs,[16] and calculation of the ligand−receptor interaction energies using the ANAL program of AMBER 8 was employed for each selected candidate.

Molecular Dynamics Simulations. In this work, all MD simulations were performed using the Amber 8 program[16] on a 68-CPU Dawning TC4000L cluster (Beijing, China). The generalized Born solvation model[17] in macromolecular simulations was used instead of explicit water. Temperature was set at 300 K with the cutoff distance of 12 Å used for unbounded interaction. The ff99 force field (Parm99)[18] was applied throughout the energy minimization and MD simulations.

A stepwise equilibration process was performed on each screened candidate complex structure by gradually reducing the force constant from a larger 5.0 (kcal/mol)/Å^2 for restraining all heavy atoms to 0.02 (kcal/mol)/Å^2 for only heavy atoms in the backbone, each step taking 50 ps simulation time. As for the final ChTX-BK channel complex structure model, it was sufficiently equilibrated by 8 ns unrestrained MD simulations to introduce enough flexibility for both the channel and the toxin peptide.

Calculation of Binding Free Energy by MM-GBSA. In the MM-GBSA of AMBER 8.0,[17] the binding free energy of A + B → AB is calculated using the following thermodynamic cycle:

$$\begin{array}{ccccc} A_{aqu} & + & B_{aqu} & \xrightarrow{\Delta G_{binding}} & AB_{aqu} \\ \downarrow -\Delta G^{A}_{solv} & & \downarrow -\Delta G^{B}_{solv} & & \downarrow -\Delta G^{AB}_{solv} \\ A_{gas} & + & B_{gas} & \xrightarrow{\Delta G_{gas}} & AB_{gas} \end{array}$$

$$\Delta G_{binding} = \Delta G_{gas} - \Delta G^{A}_{solv} - \Delta G^{B}_{solv} + \Delta G^{AB}_{solv}$$

$$= \Delta H_{gas} - T\Delta S - \Delta G^{A}_{GBSA} - \Delta G^{B}_{GBSA} + \Delta G^{AB}_{GBSA}$$

$$= \Delta H_{gas} - T\Delta S + \Delta\Delta G_{GB} + \Delta\Delta G_{SA} \quad (1)$$

$$\Delta H_{gas} \approx \Delta E_{gas} = \Delta E_{intra} + \Delta E_{elec} + \Delta E_{vdW} \quad (2)$$

$$\Delta\Delta G_{GB} = \Delta G^{AB}_{GB} - (\Delta G^{A}_{GB} + \Delta G^{B}_{GB}) \quad (3)$$

$$\Delta\Delta G_{SA} = \Delta G^{AB}_{SA} - (\Delta G^{A}_{SA} + \Delta G^{B}_{SA}) \quad (4)$$

Where T is the temperature, S is the solute entropy, ΔG_{gas} is the interaction energy between A and B in the gas phase, and ΔG^{solv}_{A}, ΔG^{solv}_{B}, and ΔG^{solv}_{AB} are the solvation free energies of A, B, and AB, which are estimated using a GB surface area (GBSA) method.[17] That is, $\Delta G^{AB}_{solv} = \Delta\Delta G^{AB}_{GBSA} + \Delta G^{AB}_{GB} + \Delta G^{AB}_{SA}$, and so forth. ΔG_{GB} and ΔG_{SA} are the electrostatic and nonpolar term, respectively. ΔE_{bond}, ΔE_{angle}, and $\Delta E_{torsion}$ are contributions to the intramolecular energy ΔE_{intra} of the complex. E_{vdW} is van der Waals (vdW) interaction energy. Because of the constant contribution of $-T\Delta S$ for each docked complex, we quote $\Delta G^{*}_{binding}$ for $\Delta G_{binding} + T\Delta S$ in the discussion. To verify the quality and validity of the resulting ChTX-BK complexes, the relative binding free energy $\Delta G^{*}_{binding}$ was calculated by using MM-GBSA for postprocessing collected snapshots from the MD trajectories. In this work, 30 snapshots from the last 30 ps MD simulations were used for binding free energy analysis.

RESULTS AND DISCUSSION

Molecular Docking and Screening of ChTX-BK Complex Structure. Using combined computational methods and experimental information, we ever characterized interactions between several peptides (BeKm-1, maurotoxin, ADWX-1) and potassium channels (hERG, Kv1.2, Kv1.3).[6−8] In addition, we also discussed some important factors involved in the formation of stable maurotoxin-Kv1.2 complex.[8] In this work, the similar strategy was adopted to characterize the interaction between ChTX and BK channel, and the ZDOCK program[15] was applied to predict possible ChTX-BK complex structures. After energy minimization and clustering analysis of candidate complex structures, four main binding modes of ChTX-BK complex were identified with the help of experimental information.[11,12] Among the four binding modes, ChTX all used the β-sheet domain as the main binding surface, with Lys27 residue occluding the pore of BK channel (Figure 1). In addition, four turrets were in the decentralized state and had less effect on the ChTX binding.

The differences among the four binding modes mainly lied on the spatial orientations of ChTX β-sheet domain. In Mode I, the toxin β-sheet presented a flat orientation by diagonal way around the central axes of BK channel. in Mode II, the β-sheet presented a slope orientation by middle way around the central axes of channel. In Mode III, it was a flat β-sheet by middle way around the central axes of channel, in Mode IV, the β-sheet presented a slop orientation by diagonal way around the central axes of channel (Figure 1). To better discriminate among the four plausible ChTX-BK binding modes,[8] 500 ps unrestrained MD simulations followed by computational alanine-scanning method in MM-PBSA[17] were performed for complexes in all four binding modes. From the comparison of computational and experimental data of four functional residues (Figure 1 and Table 1), a ChTX-BK complex structural model from Mode I was found to be the best candidate among four binding modes. To make the obtained complex more stable and convincible, an additional 8 ns unrestrained MD simulation was preformed to enough equilibrate the ChTX-BK complex structure. The little variance of backbone root-mean-square deviation (rmsd) indicated that the system was sufficiently equilibrated at the end of the simulation (Figure 2A and B). Although there was rmsd fluctuation for ChTX-BK complex structure, such change was mainly caused by the conformational flexibility of four channel turrets.

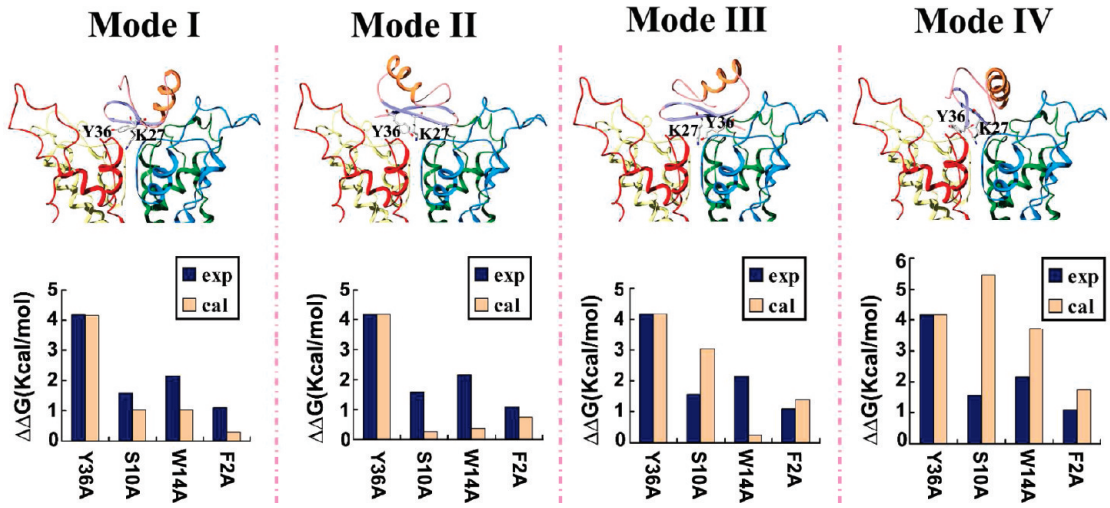

Figure 1. View of the four selected ChTX-BK channel binding modes in the individual column together with the comparison of calculated and experimental effects. Each row of figures as follows: (top) the differential spatial orientations of ChTX in complex with BK channel from four main binding modes. The most critical residues Lys^{27} and Tyr^{36} of ChTX are labeled. (bottom) The comparison of calculated and experimental effects for the four alanine mutations of ChTX on the binding affinity toward BK channel, the calculated results are normalized values of $\Delta\Delta G_{binding}$, whereas experimental results are obtained as k_bT ln [IC_{50}(mutant)/IC_{50}(wt)].

Table 1. IC_{50} Values of Wild Type and Mutants of ChTX toward BK Channel

ChTX mutant and reference	IC_{50} (nM)	IC_{50}(mut)/IC_{50}(wt)
WT[11]	8.8	1.0
F2A[11]	55	6.3
S10A[11]	120	13.6
W14A[11]	330	37.5
T23D[11]	2000	227.3
M29L[11]	1600	181.8
M29I[11]	9100	1034.1
M29K[11]	15000	1704.5
Y36A[11]	9400	1068.2
WT[12]	15	1.0
R25Q[12]	610	40.7
R34Q[12]	330	22.0
WT[19]	3.9	1.0
F266A[19]	4.2	1.1

Next, the consistency between computational and experimental alanine-scanning mutagenesis results[11,19] was further evaluated. As shown in Figure 2C, an overall high degree of correlation was found between the calculation results and the experiment data. When Tyr36 was substituted by alanine, the affinity of ChTX toward BK was reduced by over 1100 fold[11] (Table 1). In accordance with this, the calculated binding free energy ($\Delta\Delta G_{binding}$) for Y36A gave a biggest value of 4.16 kcal/mol. The decrease of binding affinity was minor when Ser10 or Trp14 was mutated to alanine[11] (Table 1), in compliance with this, the calculated $\Delta\Delta G_{binding}$ was 1.04 kcal/mol for S10A and 1.03 kcal/mol for W14A. In addition, both the Phe2 in ChTX and Phe266 in BK channel turret gave neglectable experimental and computational $\Delta\Delta G_{binding}$ values[19] (Table 1). Together, the excellent coincidence between experimental and computational data suggested that our ChTX-BK model was a reasonable structure. Based on the obtained ChTX-BK complex structure, some novel interaction information could be explored through structural analysis.

Interaction Information of ChTX Functional Dyad. The functional dyad, a pair of residues (basic and hydrophobic residues), is regarded as an important molecular determinant for toxin peptides acting on voltage-gated Kv1.x channels.[2,20] However, there are only a few functional dyads well characterized at the level of peptide-channel complex structures, such as ADWX-1 and maurotoxin (Figure 3A).[7,8]

In the obtained ChTX-BK complex structure, ChTX mainly used the functional dyad consisting of Lys27 and Tyr36 to associate BK channel (Figure 3B). This binding mode was similar to that of ChTX associating KcsA channel, which was predicted by Yu et al.[21] using protein−protein docking (Figure 3C). Consideration of the similarity in the binding mode of ChTX recognizing BK and Kv channels may clarify the reason for the equivalent blocking affinity of ChTX toward both BK and Kv1.x channel family.[22] In the obtained ChTX-BK complex, Lys27 used the well-known orientation to exert its pharmacological function by plugging its side chain into channel selectivity filter. The other Tyr36 of ChTX lay above the loops connecting selectivity filter and S6 helix in the channel C and D chains (Figure 3D). Within a contact distance of 4 Å, the Tyr36 mainly interacted with Gly291, Tyr294, and Arg301 residues located in the pore region of the channel, and even formed a hydrogen-bond with Gly291 residue (Figure 3D). Similar to the distribution of Tyr36 in ChTX, the hydrophobic Tyr32 in the functional dyad of maurotoxin is also located at the end of sequence C-terminal (Figure 3A). However, the Tyr32 side chain of maurotoxin did not lie above the loops connecting selectivity filter and S6 helix, but just stuck between the channel turret and the loop linking the selectivity filter and S6 helix (Figure 3E). Interestingly, the Phe24 side chain in the functional dyad of ADWX-1 peptide (Figure 3A) also adopted similar orientation to that of Tyr32 in maurotoxin.[7] Such difference in the interaction information from the functional dyads suggests that there are likely diverse recognizing mechanisms of functional dyads among scorpion toxins and their analogs.

Novel Orientation of Arg25 Residue in ChTX. As shown in Figure 3A, there is a conserved arginine residue close to the pore-blocking lysine residue, among ChTX, AgTX2, and ADWX-1 peptides. These arginine residues

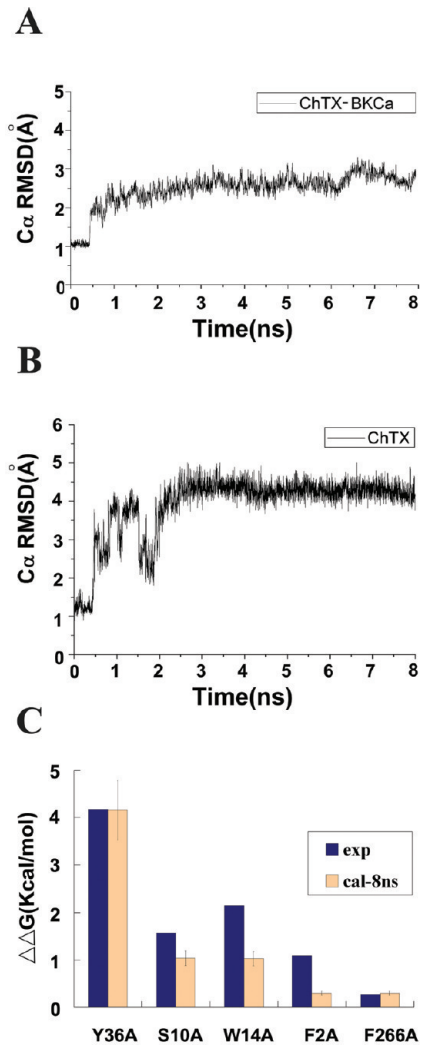

Figure 2. Stability and validity of the final ChTX-BK complex. (A) Root-mean-square deviations (Å) of the α-carbons of the final ChTX-BK complex from the starting complex along the 8 ns MD simulations. (B) Root-mean-square deviations (Å) of the α-carbons of the toxin ChTX from the starting conformation along the 8 ns MD simulations. (C) Calculated and experimental effects for 5 single alanine mutations on the blocking affinity of ChTX toward BK channel. The calculated results are normalized values of $\Delta\Delta G_{binding}$, whereas experimental results are obtained as k_bT ln [IC_{50}(mutant)/IC_{50}(wt)].

were found important for peptide binding affinity toward potassium channels,[23] however, their arrangements have a little difference. In ChTX, there is only Gly26 residue between Arg25 and Lys27. In AgTX2 and ADWX-1, there are two residues (Phe and Gly) between the conserved arginine residue and pore-blocking lysine residue. In this work, the ChTX-BK complex structure showed that this discrepancy in arginine distribution further led to the difference of recognizing mechanism for different peptides.

In ChTX-BK complex structure model, the side chain of Arg25 was located between loops formed by channel B and C chains (Figure 4A). Within a contact distance of 4 Å, the Arg25 mainly contacted Tyr290 (B chain), Gly289 (C chain), Gly291 (C chain), Val293 (C chain), and Tyr294 (C chain) with four hydrogen bonds. Such residue−residue interaction might explain the experimental data that the substitution of glutamine for Arg25 decreased ChTX binding affinity by about 41-fold[12] (Table 1). In the ADWX-1-Kv1.3 complex obtained from our previous work,[7] the critical Arg23 residue formed an electrostatic interaction with the conserved Asp386 residue on pore helix of Kv1.3 channel (Figure 4B).[7] Such recognizing mechanism difference of the conserved arginine residue is just caused by their different location in ChTX and ADWX-1 sequences. Unlike Arg23 residue in ADWX-1, Arg25 residue of ChTX is closer to the pore-blocking Lys27 residue so that Arg25 side chain is likely unable to contact the distant and conserved Glu276 of BK channel in the pore helix.

Interaction Information of Other Residues in ChTX. Besides the chemical information of important Arg25, Lys27, and Tyr36 residues, the ChTX-BK complex model also presented related interaction information, which could be used to explain experimental data of other residues in ChTX.

In both the N-terminal loop and α-helical domains, the functional residues were mainly distributed at the beginning of α-helical domain. As shown in Figure 5A, the Ser10 in ChTX contacted the Asp292 near the selectivity filter of BK channel through polar interaction, and the other Trp14 residue in the helical domain of ChTX peptide interacted with Lys296 through nonpolar interaction. The disappearance of the polar or nonpolar interaction would lead to about 13- or 37-fold decrease of ChTX binding affinity when Ser10 or Trp14 was replaced by alanine in ChTX, respectively[11] (Table 1). It seems the common feature that one or two functional residues are located between N-terminal loop and α-helical domains when scorpion toxin peptides adopt the β-sheets as the main channel-interacting surface. In the AgTX2 and ADWX-1 peptides, the Ser11 in AgTX2 and Arg11 in ADWX-1 were also found to be important for peptide binding affinity.[7,24]

Among all mutagenesis data of ChTX, the replacement of Met29 by leucine, isoleucine, and lysine residues led to about 180-, 1034-, and 1700-fold decrease of ChTX pharmacological activities[11] (Table 1). These perplexed data could be well explained by the ChTX-BK complex model. As shown in Figure 5B, the side chain of Met29 just faced the backbone of Gly291-Asp292-Val293 residues in BK channel. Simultaneously, the Met29 is also close to the important Arg34 residue in ChTX peptide, therefore, such local environment of Met29 seemed highly unfavorable to the more hydrophobic leucine, isoleucine, or the basic lysine residues. In addition, the Arg34 residue of ChTX was found to form salt-bridges with Asp292 and hydrogen bonded with Gly291 in BK channel (Figure 5B). This strong polar interaction was in line with the drop of ChTX affinity on BK channel for about 22-fold when Arg34 was mutated into glutamine residue[12] (Table 1).

Conformational Change of ChTX Induced By the Interaction with BK Channel. Obvious structural rearrangements have ever been found to associate the interaction between scorpion toxins and K^+ channels.[6,8,25,26] In this work, we also observed conformational change during the formation of the stable ChTX-BK channel complex (Figure 6). By analyzing the whole MD trajectories, a large Cα rmsd of 4.69 Å was detected for the bound and unbound ChTX, with the three pairs of disulfide bridges well kept (Figure 6A). Such rmsd value was much larger than the value of 2.75 Å between the bound and unbound MTX peptide in our previous work.[8] The most remarkable transformation occurred in the Gln1-Val5 segment located

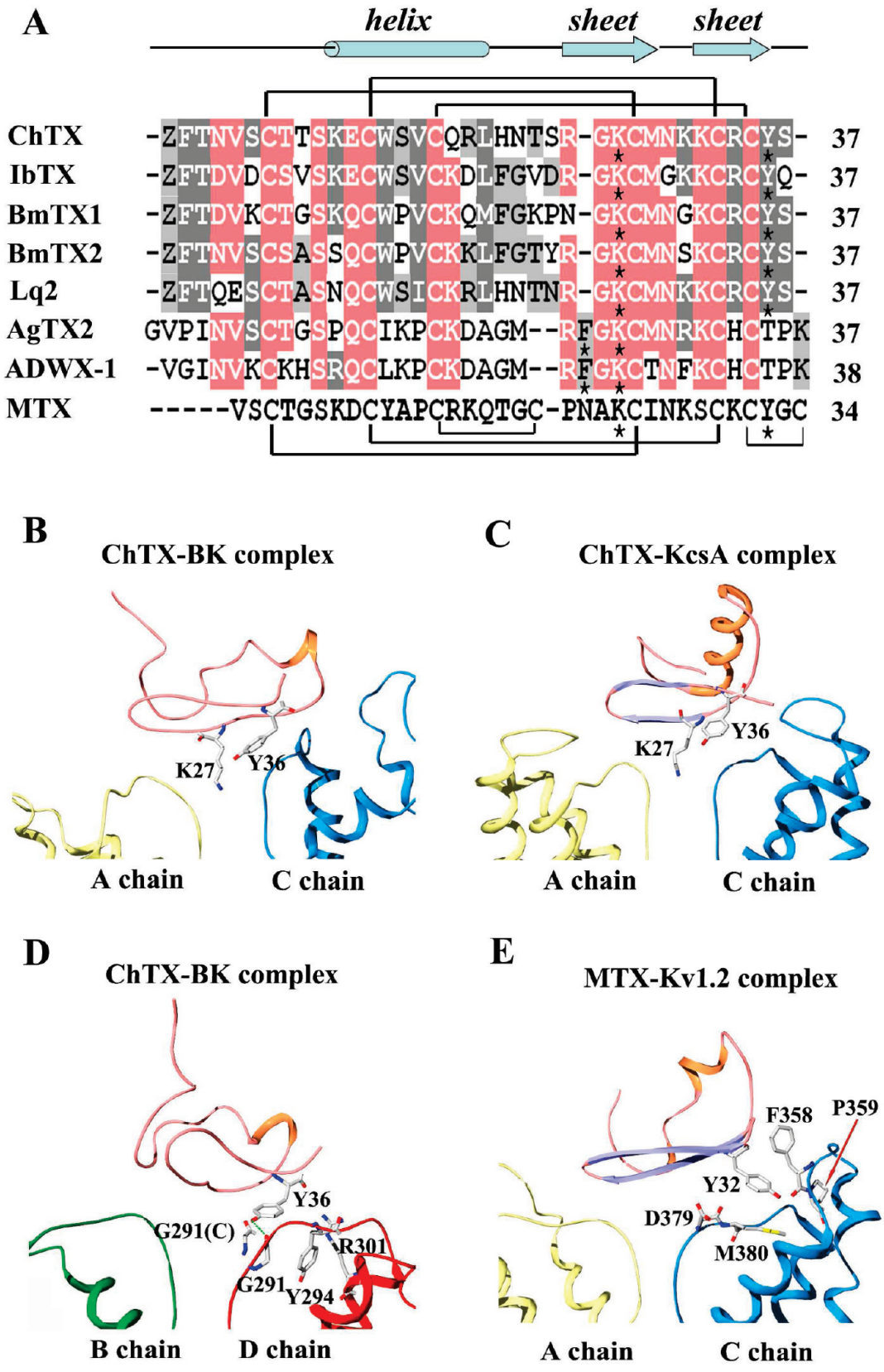

Figure 3. Interaction details of the functional dyad in ChTX. (A) Sequence alignment of ChTX with iberiotoxin, BmTX1, BmTX2, Lq2, AgTX2, ADWX-1, and MTX. The functional dyad residues for each toxin are labeled by asterisks, and the disulfide bridges are shown by lines. (B) The ChTX-BK complex. ChTX adopted the functional dyad consisting of Lys^{27} and Tyr^{36} to associate with BK channel. (C) The ChTX-KcsA complex (PDB code: 2A9H) predicted by Yu et al.,[21] ChTX adopted the functional dyad consisting of Lys^{27} and Tyr^{36} to associate with KcsA channel. (D) The Tyr^{36} of ChTX was surrounded by Gly^{291} on C chain, Gly^{291}, Tyr^{294}, and Arg^{301} residues on D chain of BK channel. (E) The MTX-Kv1.2 complex from our previous work.[8] The Tyr^{32} of MTX stuck between the channel turret and the loop linking the selectivity filter and S6 helix.

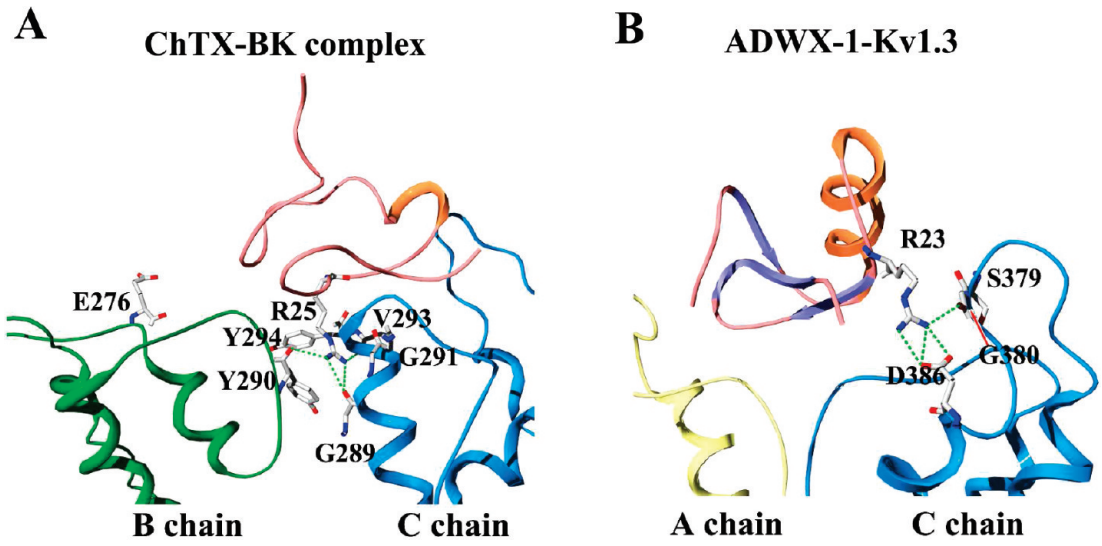

Figure 4. Interaction details of arginine residues in ChTX and ADWX-1. (A) Interaction details of Arg^{25} in ChTX-BK complex. The Arg^{25} mainly contacted Tyr^{290} (B chain), Gly^{289} (C chain), Gly^{291} (C chain), Val^{293} (C chain), and Tyr^{294} (C chain) of BK channel with four hydrogen bonds. (B) Interaction details of Arg^{23} in ADWX-1-Kv1.3 complex, which is from our previous work.[7] The Arg^{23} residue formed a strong electrostatic interaction with Asp^{386} residue on pore helix of Kv1.3 channel.

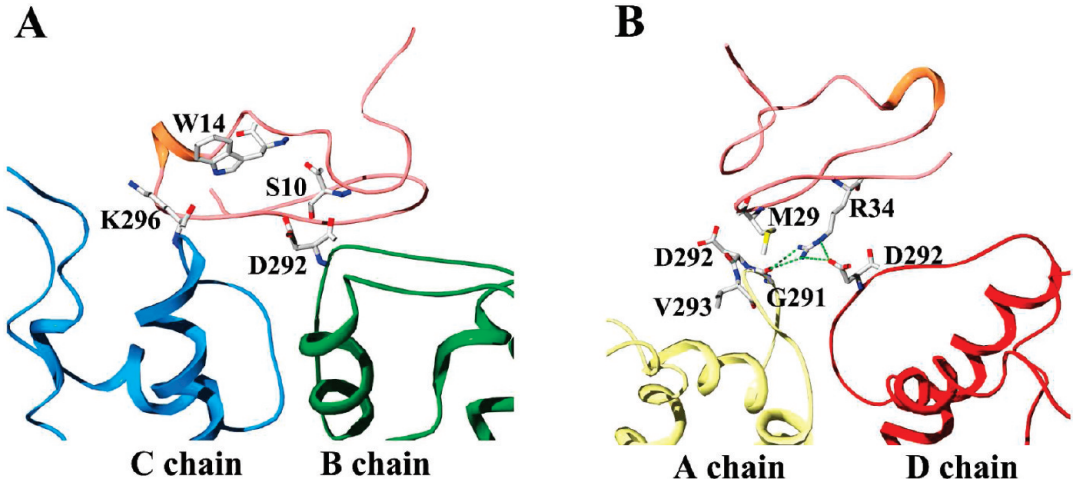

Figure 5. Interaction details of other residues in ChTX. (A) within a distance of 4 Å, the Ser^{10} and Trp^{14} of ChTX contacted with Asp^{292} and Lys^{296} residues on the channel vestibule, respectively. (B) The side chain of Met^{29} faced the backbone of Gly^{291}-Asp^{292}-Val^{293} residues in BK channel. The Arg^{34} residue of ChTX formed salt-bridges with Asp^{292} and hydrogen bonded with Gly^{291} in BK channel.

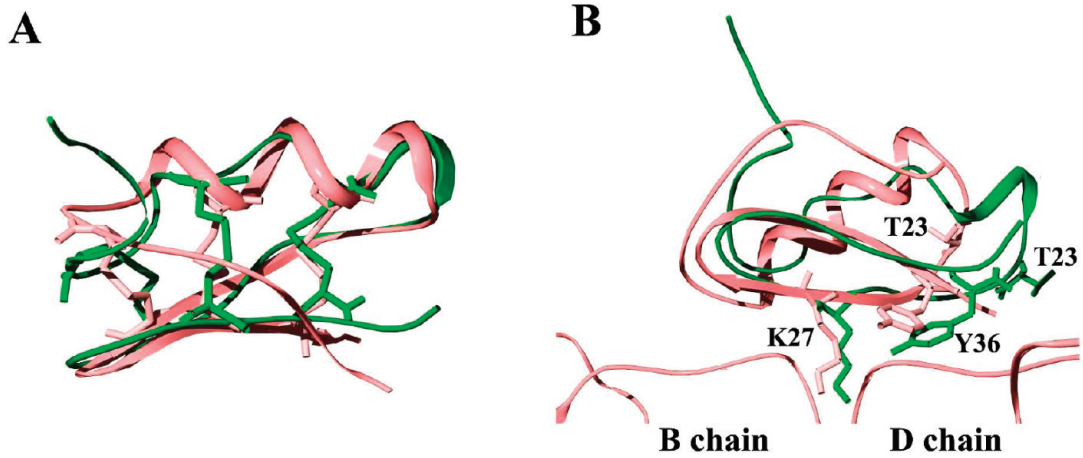

Figure 6. Conformational change induced by ChTX-BK channel interaction. (A) Ribbon view of comparison between unbound and bound ChTX, with the three pairs of disulfide bridges in solid bonds. (B) Orientation difference of ChTX from the starting conformation and the equilibrated conformation above channel outer vestibule, with side chains of Lys^{27}, Tyr^{36}, and Thr^{23} marked in solid bonds. The free ChTX and BK channel are colored pink, and ChTX after MD simulations is colored green.

far from the interaction surface, indicating a high flexibility in the N-terminal of the ChTX peptide (Figure 6B). At the beginning of the MDs, the backbone of the Gln1-Val5 segment pointed toward the pore region of the BK

channel. After 8 ns MDs, this segment turned 180° and adopted a totally reverse direction by pointing away from the channel, which might suggest that the Gln1-Val5 of ChTX was unfavorable to the channel pore region residues. The loop connecting α-helix and β-sheet also presented some extent of flexibility (Figure 6B). For example, the backbone of Thr23 tended to be much closer to the channel vestibule during the recognition process, which could be related with the experimental data that T23D mutant of ChTX caused a 230-fold decreased BK channel binding affinity[11] (Table 1).

On the BK channel side, since the four turrets hardly took part in the peptide association, their conformation almost kept unchanged in a decentralized state, and the previous alanine mutation of four Phe266 residues in the turret supported this finding[19] (Table 1). In view of the sequence conservation of pore regions between Kv1.x and BK channels, the noninvolvement of BK channel turret in the binding process could also explain the fact that ChTX and other ChTX-like peptides could not distinguish between BK and Kv1.x channels.[22,27,28]

CONCLUSIONS

A reasonable structure of ChTX peptide in complex with BK channel was obtained by ZDOCK, computational alanine-scanning analysis and MD simulations. This ChTX-BK complex structure provided much helpful structural information on their interactions. With β-sheet domain as the main binding surface, the ChTX peptide used the Lys27 residue to occlude the pore of BK channel. Tyr36, another crucial residue of ChTX, lay above the loops connecting selectivity filter and S6 helix in the channel C and D chains, forming a hydrogen bond with Gly291 of BK channel. The four hydrogen bonds between Arg25 of ChTX and Gly289, Val293 and Tyr294 on C chain of BK channel revealed that Arg25 was an important residue for the binding process, and its novel orientation made its recognition mechanism distinct from the conserved arginine residues in other peptides. Furthermore, considerable conformational transformation induced by the interaction strongly implies that the binding of ChTX toward BK channel was a dynamic process of conformational rearrangements. In all, our reasonable ChTX-BK complex structure revealed the mechanic basis of ChTX recognizing BK channel, which would present much information on the diverse scorpion toxin-potassium channel interactions and accelerate the molecular design of toxin-based specific inhibitors.

ACKNOWLEDGMENT

This work was supported by grants from the National Natural Sciences Foundation of China (Number: 30530140 and 30770519) and the Basic Project of Ministry of Science and Technology of China (Number 2007FY210800).

REFERENCES AND NOTES

(1) Rodriguez de la Vega, R. C.; Merino, E.; Becerril, B.; Possani, L. D. Novel interactions between K^+ channels and scorpion toxins. *Trends Pharmacol. Sci.* **2003**, *24* (5), 222–7.
(2) Rodriguez de la Vega, R. C.; Possani, L. D. Current views on scorpion toxins specific for K^+-channels. *Toxicon* **2004**, *43* (8), 865–75.
(3) Hidalgo, P.; MacKinnon, R. Revealing the architecture of a K^+ channel pore through mutant cycles with a peptide inhibitor. *Science* **1995**, *268* (5208), 307–10.
(4) MacKinnon, R.; Cohen, S. L.; Kuo, A.; Lee, A.; Chait, B. T. Structural conservation in prokaryotic and eukaryotic potassium channels. *Science* **1998**, *280* (5360), 106–9.
(5) Lu, Z.; Klem, A. M.; Ramu, Y. Ion conduction pore is conserved among potassium channels. *Nature* **2001**, *413* (6858), 809–13.
(6) Yi, H.; Cao, Z.; Yin, S.; Dai, C.; Wu, Y.; Li, W. Interaction simulation of hERG K^+ channel with its specific BeKm-1 peptide: insights into the selectivity of molecular recognition. *J. Proteome Res.* **2007**, *6* (2), 611–20.
(7) Han, S.; Yi, H.; Yin, S.; Chen, Z. Y.; Liu, H.; Cao, Z.; Wu, Y.; Li, W. Structural basis of a potent peptide inhibitor designed for Kv1.3 channel, a therapeutic target of autoimmune disease. *J. Biol. Chem.* **2008**, *283* (27), 19058–65.
(8) Yi, H.; Qiu, S.; Cao, Z.; Wu, Y.; Li, W. Molecular basis of inhibitory peptide maurotoxin recognizing Kv1.2 channel explored by ZDOCK and molecular dynamic simulations. *Proteins* **2008**, *70* (3), 844–54.
(9) Yin, S.; Jiang, L.; Yi, H.; Han, S.; Yang, D.; Liu, M.; Liu, H.; Cao, Z.; Wu, Y.; Li, W. Different residues in channel turret determining the selectivity of ADWX-1 inhibitor peptide between Kv1.1 and Kv1.3 channels. *J. Proteome Res.* **2008**, *7* (11), 4890–7.
(10) Gimenez-Gallego, G.; Navia, M. A.; Reuben, J. P.; Katz, G. M.; Kaczorowski, G. J.; Garcia, M. L. Purification, sequence, and model structure of charybdotoxin, a potent selective inhibitor of calcium-activated potassium channels. *Proc. Natl. Acad. Sci. U.S.A.* **1988**, *85* (10), 3329–33.
(11) Stampe, P.; Kolmakova-Partensky, L.; Miller, C. Intimations of K^+ channel structure from a complete functional map of the molecular surface of charybdotoxin. *Biochemistry* **1994**, *33* (2), 443–50.
(12) Park, C. S.; Miller, C. Mapping function to structure in a channel-blocking peptide: electrostatic mutants of charybdotoxin. *Biochemistry* **1992**, *31* (34), 7749–55.
(13) Gan, G.; Yi, H.; Chen, M.; Sun, L.; Li, W.; Wu, Y.; Ding, J. Structural Basis for Toxin Resistance of β4-Associated Calcium-activated Potassium (BK) Channels. *J. Biol. Chem.* **2008**, *283* (35), 24177–84.
(14) Bontems, F.; Gilquin, B.; Roumestand, C.; Menez, A.; Toma, F. Analysis of side-chain organization on a refined model of charybdotoxin: structural and functional implications. *Biochemistry* **1992**, *31* (34), 7756–64.
(15) Chen, R.; Li, L.; Weng, Z. ZDOCK: an initial-stage protein-docking algorithm. *Proteins* **2003**, *52* (1), 80–7.
(16) Case, D. A.; Darden, T. A.; Cheatham, T. E., III; Simmerling, C. L.; Wang, J.; Duke, R. E.; Luo, R.; Merz, K. M.; Wang, B.; Pearlman, D. A.; Crowley, M.; Brozell, S.; Tsui, V.; Gohlke, H.; Mongan, J.; Hornak, V.; Cui, G.; Beroza, P.; Schafmeister, C.; Caldwell, J. W.; Ross, W. S.; Kollman, P. A. In *Amber 8*; University of California: San Francisco, CA, 2004; pp 9−174.
(17) Darden, T. A.; Case, D. A. Molecular dynamics simulations of nucleic acids with a generalized born solvation model. *J. Am. Chem. Soc.* **2000**, *122* (11), 2489–98.
(18) Wang, J. M.; Cieplak, P.; Kollman, P. A. How well does a RESP (restrained electrostatic potential) model do in calculating the conformational energies of organic and biological molecules. *J. Comput. Chem.* **2000**, *21* (12), 1049–74.
(19) Yao, J.; Li, H.; Gan, G. L.; Wu, Y.; Ding, J. P. Residue Phe266 in S5-S6 loop is not critical for charybdotoxin binding to Ca^{2+}-activated K^+ (mSlo1) channels. *Acta. Pharmacol. Sin.* **2006**, *27* (7), 945–9.
(20) Mouhat, S.; De Waard, M.; Sabatier, J. M. Contribution of the functional dyad of animal toxins acting on voltage-gated Kv1-type channels. *J. Pept. Sci.* **2005**, *11* (2), 65–8.
(21) Yu, L.; Sun, C.; Song, D.; Shen, J.; Xu, N.; Gunasekera, A.; Hajduk, P. J.; Olejniczak, E. T. Nuclear magnetic resonance structural studies of a potassium channel-charybdotoxin complex. *Biochemistry* **2005**, *44* (48), 15834–41.
(22) Giangiacomo, K. M.; Sugg, E. E.; Garcia-Calvo, M.; Leonard, R. J.; McManus, O. B.; Kaczorowski, G. J.; Garcia, M. L. Synthetic charybdotoxin−iberiotoxin chimeric peptides define toxin binding sites on calcium-activated and voltage-dependent potassium channels. *Biochemistry* **1993**, *32* (9), 2363–70.
(23) Giangiacomo, K. M.; Ceralde, Y.; Mullmann, T. J. Molecular basis of α-KTx specificity. *Toxicon* **2004**, *43* (8), 877–86.
(24) Ranganathan, R.; Lewis, J. H.; MacKinnon, R. Spatial localization of the K^+ channel selectivity filter by mutant cycle-based structure analysis. *Neuron* **1996**, *16* (1), 131–9.
(25) Huang, X.; Dong, F.; Zhou, H. X. Electrostatic recognition and induced fit in the κ-PVIIA toxin binding to Shaker potassium channel. *J. Am. Chem. Soc.* **2005**, *127* (18), 6836–49.

(26) Lange, A.; Giller, K.; Hornig, S.; Martin-Eauclaire, M. F.; Pongs, O.; Becker, S.; Baldus, M. Toxin-induced conformational changes in a potassium channel revealed by solid-state NMR. *Nature* **2006**, *440* (7086), 959–62.

(27) Crest, M.; Jacquet, G.; Gola, M.; Zerrouk, H.; Benslimane, A.; Rochat, H.; Mansuelle, P.; Martin-Eauclaire, M. F. Kaliotoxin, a novel peptidyl inhibitor of neuronal BK-type Ca^{2+}-activated K^+ channels characterized from Androctonus mauretanicus mauretanicus venom. *J. Biol. Chem.* **1992**, *267* (3), 1640–7.

(28) Romi-Lebrun, R.; Lebrun, B.; Martin-Eauclaire, M. F.; Ishiguro, M.; Escoubas, P.; Wu, F. Q.; Hisada, M.; Pongs, O.; Nakajima, T. Purification, characterization, and synthesis of three novel toxins from the Chinese scorpion Buthus martensi, which act on K^+ channels. *Biochemistry* **1997**, *36* (44), 13473–82.

CI900025N